# Calculation of Near and Far Acoustic Fields Due to a Spinning Vortex Pair in Free Field

Sam-Ok Koo*, Ki-Wahn Ryu† and Duck-Joo Lee‡

# 자유흐름장 내의 회전하는 와류쌍에 의한 근거리 및 원거리 음장해석

구삼옥 유기완 이덕주

자유흐름장에 놓여 있는 회전 와류쌍을 음원으로 갖는 비정상 유동장에서 사극음원이 음장에 미치는 효과를 알아보기 위해 이차원 음장 수치해석을 시도하였다. 비압축성 유동장에 대한 비정상 수력정보를 기반으로 오일러식에서 교란 압축성 소음항을 도출하였다. 원거리 자유 경계면은 비반사 경계조건을 이용하여 매우 안정된 해를 얻을 수 있었다. 계산된 결과들은 MAE 방법과 비교하여 정확도를 입증하였다. 본 연구를 통해 비압축성 압력교란을 원천항으로 하여 물체가 존재하지 않는 경우에도 사극음원에 의한 음장을 수치적으로 계산이 가능함을 입증하였다.

Key Words : CAA (전산공력음향학), Spinning Vortex (회전와류), Nonreflecting BC (비반사 경계조건), Hydrodynamic Density (수력밀도), Near Field (근거리), Far Field (원거리)

## Nomenclature

$\mathbf{A}, \mathbf{B}$ = Jacobian matrices
$a_0$ = ambient speed of sound
$b$ = vortex position in complex domain
$f$ = frequency
$H_2^{(2)}(kr)$ $2^{nd}$ kind of Hankel function of order 2
$i$ = imaginary number
$\mathbf{E}, \mathbf{F}$ = flux vectors in the $\xi$ and $y$ directions
$k$ = wave number $(2\omega/a_0)$
$M_r$ = rotating Mach number
$p$ = hydrodynamic pressure
$\bar{p}$ = time-mean hydrodynamic pressure
$p'$ = acoustic pressure
$\mathbf{Q}$ = vector of conservative variables
$r_c$ = core radius of the Scully vortex model
$r_0$ = radius of rotation of vortex pair
$\mathbf{S}, \mathbf{S}_1$ = source term in acoustic equation
$T$ = period of rotation (spinning vortex pair)
$t$ = time
$\mathbf{U}$ = vector of primitive variables
$u, v$ = hydrodynamic velocity components
$u', v'$ = acoustic velocity components
$\mathbf{X}, \mathbf{Y}$ = eigen-vector matrix of $\mathbf{A}$ and $\mathbf{B}$
$x, y$ = Cartesian coordinates
$\Gamma$ = Circulation (+: counterclockwise)
$\gamma$ = ratio of specific heat
$\Delta t$ = time step
$\theta$ = angular argument
$\lambda$ = wave length
$\Lambda, \mathbf{M}$ = diagonal matrix of $\mathbf{A}$ and $\mathbf{B}$
$\rho_0$ = ambient density
$\rho_1$ = hydrodynamic density correction
$\rho'$ = acoustic density
$\sigma_t$ = weighting factor in time stepping
$\Phi$ = complex velocity potential
$\omega$ = angular velocity

*선임 연구원, 한국항공우주 연구소
†학생회원, 한국과학기술원 항공우주공학과
‡정회원, 한국과학기술원 항공우주공학과

## 1. Introduction

Studies on sound generation by unsteady flowfields in the presence or in the absence of a body are important to the understanding and solving of many noise problems of practical interest; for example, blade-vortex interaction, edge tones, and jet noise. The motions of vorticity are considered to be directly related to the source of sound generated by vortical flows. These phenomena have been studied both theoretically [1 – 6] and numerically [7 – 14] by many researchers.

Hardin and Pope [11, 12] proposed a computational aeroacoustics technique, where they split the Euler equations into hydrodynamic terms and perturbed acoustic terms. The novelty of their approach is found in the introduction of a new variable named 'hydrodynamic density fluctuations', which is the basic difference in the formulation of governing equations from others [9, 10]. They applied the technique to the problems of a pulsating and an oscillating sphere, which were acting as a monopole or a dipole source with sound-generating body surfaces. The main advantage of this method is that one can use the inco,pressible flow solution to calculate the acoustic fields at low Mach number flows.

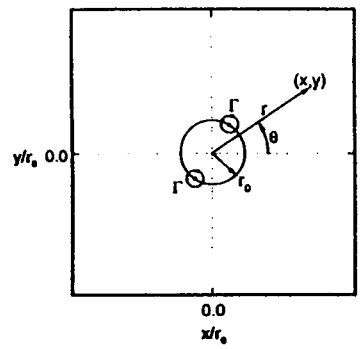


Fig. 1 Schematic diagram of flow configuration.

In the present paper, we numerically studied the sound generation by purely quadrupole sources. The acoustic field induced by a spinning vortex pair is calculated. The spinning vortex pair has analytic solutions and represents the basic acoustic field generated by turbulent shear flows, jet flows, edge tones, etc. The goals of this study are to verify the applicability of the CAA (Computational Aero-Acoustics) technique to calculate the sound generated by a purely unsteady vortical flow, to study associated numerical problems such as boundary conditions and vortex models, and to investigate the basic physics of compressible sound generation due to the incompressible flow fluctuations. The hydrodynamic terms are obtained from the analytic solutions of the spinning vortex pair in this numerical study. It is verified that the acoustic field calculated numerically agrees well with the analytical one obtained by matched asymptotic expansion (MAE).

## 2. Descriptions of the Flow and Acoustic Field

### 2.1 Flow Field

The flow field induced by a spinning vortex pair can be assumed as inviscid and incompressible. As shown in Fig. 1, The two point-vortices, separated by a distance of $2r_0$, with circulation intensity of $\Gamma$, has a period $T = 8\pi^2 r_o^2/\Gamma$, rotating speed $\omega = \Gamma/(4\pi r_0^2)$, wave length $\lambda = \pi a_0/\omega$, and rotating Mach number $M_r = \Gamma/(4\pi r_0 a_0)$.

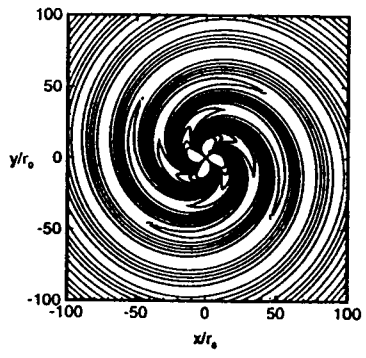


Fig. 2 Analytic acoustic pressure contour for $\Gamma/a_0 r_0 = 1.0, M_r = 0.0796$.

### 2.2 Acoustic Field by MAE

Theoretical analysis by the method of matched asymptotic expansions (MAE) for spinning vortex pair was first performed by Müller and Obermeier [2] and is also discussed in Obermeier [3]. In the method of MAE, the solution of the equations for incompressible motion in the flow domain and a homogeneous compressible wave equation in the acoustic field are matched in an intermediate domain such a way as to give an asymptotic valid solution.

The incompressible, inviscid flow, which can also be considered as the inner solution of the acoustic field, induced by a pair of vortices can be expressed by a complex potential function $\Phi(z,t)$. Let $z = re^{i\theta}$, and $b = r_0 e^{i\omega t}$. For $|z/b| >> 1$, the approximated complex potential function can be approximated by

$$\Phi(z,t) \approx \frac{\Gamma}{\pi i} ln(z) - \frac{\Gamma}{2\pi i}(\frac{b}{z})^2 \qquad (1)$$

The outer acoustic field, which is the purturbed compressible flowfield, is governed by the homogeneous wave equation

$$\nabla^2\Phi - \frac{1}{a_0^2}\frac{\partial^2\Phi}{\partial t^2} = 0 \qquad (2)$$

With appropriate matching conditions and harmonic assumptions, a matched asymptotic expansion solution of the complex potential representing the leading quadrupole term is obtained as

$$\Phi(z,t) = \frac{\Gamma k^2 r_0^2}{8} H_2^{(2)}(kr) e^{-i2(\theta-\omega t)} \qquad (3)$$

where $k = 2\omega/a_0$.

The far field solution for the acoustic pressure can be obtained from Eq. (3) as

$$p'(r) = \frac{\rho_0 \Gamma^4}{64\pi^3 r_0^4 a_0^2} H_2^{(2)}(kr) \qquad (4)$$

A typical contour plot of above equation is a double spiral pattern of a rotating quadrupole as shown in Fig. 2.

### 2.3 Vortex Core Model

In the numerical analysis for the acoustic field due to spinning vortices, a vortex-core model is required to avoid the singularity at the center of the vortex. Two different vortex-core models are investigated in the present study: the Rankine and the Scully models [16]. The two models are described as follows:

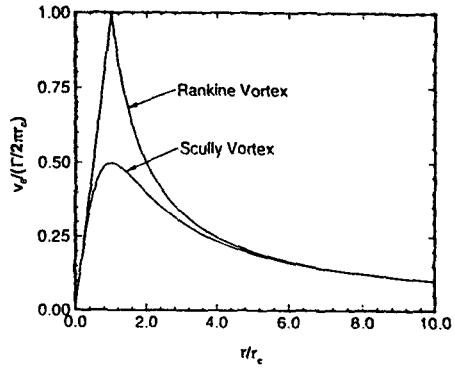


Fig. 3 Vortex velocity profiles around core.

Rankine model;

$$V_\theta = \begin{cases} \frac{\Gamma r}{2\pi r_c^2} & (0 \le r \le r_c) \\ \frac{\Gamma}{2\pi r} & (r \ge r_c) \end{cases} \qquad (5)$$

Scully model;

$$V_\theta = \frac{\Gamma r}{2\pi(r_c^2 + r^2)} \qquad (6)$$

where $V_\theta$ is the tangential velocity, $r$ is a radial distance from the vortex center, and $r_c$ is the core radius. The tangential velocity distributions of the two models are compared in Fig. 3. The Scully vortex model has smoother velocity distribution than the Rankine vortex model.

## 3. Governing Equations

To derive the two-dimensional acoustic equations from the compressible flow governing equations, let us split the velocity, pressure and

density terms into hydrodynamic terms and fluctuation terms respectively as belows:

$$\begin{aligned} \tilde{u} &= u + u' \\ \tilde{v} &= v + v' \\ \tilde{p} &= p + p' \\ \tilde{\rho} &= \rho_0 + \rho_1 + \rho' \end{aligned} \tag{7}$$

where $\rho', u', v'$ and $p'$ are the perturbed compressible acoustic density, velocities and pressure respectively; and the variables of $u, v$, and $p$ are the incompressible hydrodynamic solutions of time-dependent velocity components, and pressure, respectively. The variable $\rho_1$ is the key parameter, which relates the incompressible hydrodynamic flow field as the sound source to the compressible acoustic field. The parameter $\rho_1$, defined as the 'hydrodynamic density', is the density fluctuation induced by the hydrodynamic pressure fluctuation in the flow field. The quantity is defined by the isentropic relation as [12]:

$$\rho_1 = \frac{1}{a_0^2}(p - \bar{p}) \tag{8}$$

where

$$\bar{p} = \lim_{T\to\infty} \frac{1}{T} \int_0^T p dt$$

The hydrodynamic pressure $p$ is obtained by the unsteady Bernoulli equation as:

$$p = p_0 - \rho_0 \frac{\partial \Phi}{\partial t} - \frac{1}{2}\rho_0(u^2 + v^2) \tag{9}$$

where $\rho_0$ and $p_0$ are the constant quantities in the flow field.

From the above relations, the perturbed acoustic equations derived from the Euler equations for two-dimensional acoustic fields induced by unsteady, inviscid flow can be expressed in a non-dimensional generalized curvilinear coordinates form as:

$$\frac{\partial \mathbf{Q}}{\partial t} + \frac{\partial \mathbf{E}}{\partial x} + \frac{\partial \mathbf{F}}{\partial y} = -\mathbf{S} \tag{10}$$

where

$$\mathbf{Q} = \begin{bmatrix} \rho' \\ \hat{\rho}u' + \rho' u \\ \hat{\rho}v' + \rho' v \end{bmatrix}$$

$$\mathbf{E} = \begin{bmatrix} \hat{\rho}u' + \rho' u \\ \hat{\rho}(uu' + u'u) + \rho' uu + p' \\ \hat{\rho}(vu' + v'u) + \rho' vu \end{bmatrix}$$

$$\mathbf{F} = \begin{bmatrix} \hat{\rho}v' + \rho' v \\ \hat{\rho}(uv' + u'v) + \rho' uv \\ \hat{\rho}(vv' + v'v) + \rho' vv + p' \end{bmatrix}$$

$$\mathbf{S} = \begin{bmatrix} \frac{\partial}{\partial t}(\rho_1) + \frac{\partial}{\partial x}(\rho_1 u) + \frac{\partial}{\partial y}(\rho_1 v) \\ \frac{\partial}{\partial t}(\rho_1 u) + \frac{\partial}{\partial x}(\rho_1 uu) + \frac{\partial}{\partial y}(\rho_1 uv) \\ \frac{\partial}{\partial t}(\rho_1 v) + \frac{\partial}{\partial x}(\rho_1 vu) + \frac{\partial}{\partial y}(\rho_1 vv) \end{bmatrix}$$

where $\hat{\rho} = 1 + \rho_1 + \rho'$.

The density, velocity and pressure variables in Eq. (10) are non-dimensionalized by $\rho_0$, $a_0$ and $\rho_0 a_0^2$, respectively [13, 14]. The length and time variables in Eq. (10) are non-dimensionalized by $r_0$ and $r_0/a_0$ respectively. From the isentropic relation, the pressure fluctuation can be represented as below:

$$p' = \frac{1}{\gamma}(1 + \rho_1 + \rho')^\gamma - p \tag{11}$$

## 4. Numerical Procedure

We used the non-reflecting boundary conditions based on the impedence condition on the free field boundary to account for the oblique wave on the free boundary. Thompson's technique [15] for a Cartesian coordinates system is used to obtain the density fluctuation.

First, to apply the boundary conditions, Eq. (10) is linearized and recast in the following form:

$$\mathbf{Q}_1 \frac{\partial \mathbf{U}}{\partial t} + \mathbf{E}_1 \frac{\partial \mathbf{U}}{\partial x} + \mathbf{F}_1 \frac{\partial \mathbf{U}}{\partial y} = -\mathbf{S} \tag{12}$$

where

$$\mathbf{U} = [\rho', u', v']^T$$

$$\mathbf{Q}_1 = \frac{\partial \mathbf{Q}}{\partial \mathbf{U}}, \quad \mathbf{E}_1 = \frac{\partial \mathbf{E}}{\partial \mathbf{U}}, \quad \mathbf{F}_1 = \frac{\partial \mathbf{F}}{\partial \mathbf{U}}$$

or

$$\frac{\partial \mathbf{U}}{\partial t} + \mathbf{A}\frac{\partial \mathbf{U}}{\partial x} + \mathbf{B}\frac{\partial \mathbf{U}}{\partial y} = -\mathbf{S}_1 \qquad (13)$$

where

$$\mathbf{A} = \mathbf{Q}_1^{-1}\mathbf{E}_1, \quad \mathbf{B} = \mathbf{Q}_1^{-1}\mathbf{F}_1, \quad \mathbf{S}_1 = \mathbf{Q}_1^{-1}\mathbf{S}$$

Matrices **A** and **B** can be diagonalized by the similarity transformations.

$$\mathbf{XAX}^{-1} = \Lambda, \quad \mathbf{YBY}^{-1} = \mathbf{M}$$

where the diagonal elements of $\Lambda$ and **M** are the eigen values of **A** and **B** and can easily be obtained as:

$$\Lambda = \mathrm{diag}(u-1, u, u+1)$$

$$\mathbf{M} = \mathrm{diag}(v-1, v, v+1)$$

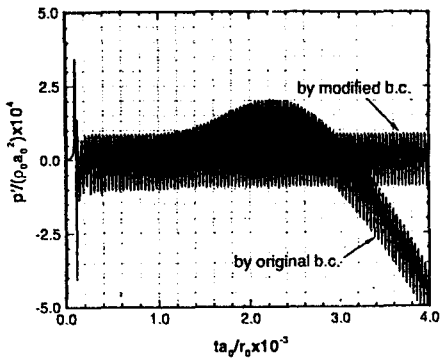


Fig. 4*a* Time history of acoustic pressure at far field for $\Gamma/a_0 r_0 = 1.0, M_r = 0.0796$.

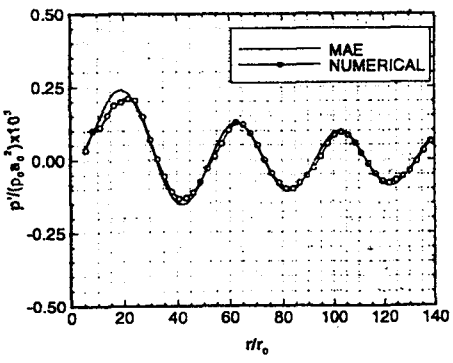


Fig. 4*b* Comparison of acoustic pressure distribution for $\Gamma/a_0 r_0 = 1.0, M_r = 0.0796$ with Scully vortex model.

Thompson's boundary conditions [15], however, have the limitation of not reproducing the outgoing acoustic signals except for planar waves. To compensate for this limitation, additional physical boundary conditions (BC) are considered here. The basic concept is that the acoustic wave radiating through the far boundary is thought to be a cylindrical plane wave. This physical condition with an isentropic assumption gives the relations [14]:

$$p' = u'_{\mathrm{radial}} = \rho' \qquad (14)$$

In the above modified BC, only $\rho'$ is calculated from Thompson's non-reflecting boundary condition, and the remaining two components are evaluated from Eq. (14).

MacCormack's predictor-corrector scheme has gained wide use and acceptance for solving time-dependent problems in fluid dynamics [17] and is used in the present study to integrate both the interior and the boundary points of Eq. (4). The time-step to meet the Courant-Friedrichs-Lewy (CFL) criterion is determined according to:

$$\Delta t = \sigma_t / \Delta t_c \qquad (15)$$

where

$$\Delta t_c = \left[ \frac{|u|}{\Delta x} + \frac{|v|}{\Delta y} + a_0 \sqrt{\frac{1}{\Delta x^2} + \frac{1}{\Delta y^2}} \right]$$

and $\sigma_t$ is a positive constant less than 1. In this study, we use $\sigma_t = 0.9$.

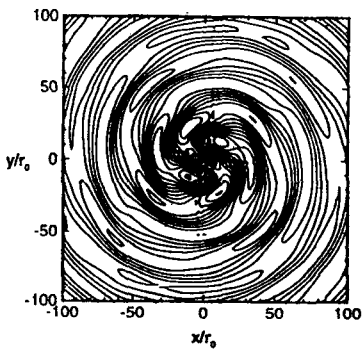


Fig. 5 Calculated acoustic pressure contour with Rankine vortex model for

$\Gamma/a_0 r_0 = 1.0, M_r = 0.0796.$

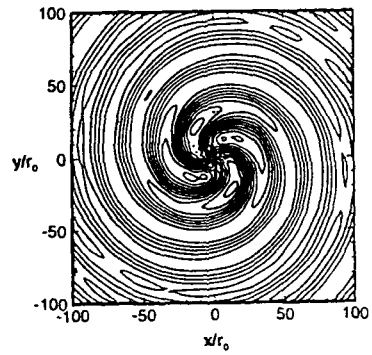


Fig. 6*a* Calculated acoustic pressure contour with Scully vortex model for $\Gamma/a_0 r_0 = 1.0, M_r = 0.0796$.

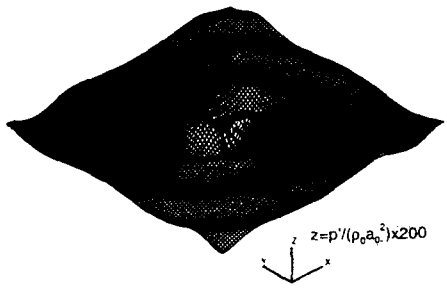


Fig. 6*b* Three-dimensional graphical view of acoustic field for $\Gamma/a_0 r_0 = 1.0, M_r = 0.0796$ with Scully vortex model.

## 5. Results and Discussions

Numerical studies are carried out for various calculation intensities $\Gamma$ and spinning radii $r_0$ of the vortex pair over a square domain of dimension $L \times L$ with an equidistance rectangular grid system. All of the calculations begin with the initial fluctuation quantities set to zero. The vortices are assumed to start spinning abruptly at time $t = 0$. Analytical solutions to the hydrodynamic flow field are evaluated at each time step over the computational domain and are used as the source term in Eq. (10).

### 5.1. Effect of Boundary Conditions

The acoustic signal propagated to a given far-field point of $x/r_0 = 100, y/r_0 = 0$ is plotted in Fig. 4*a*. No noticeable signal is observed until the nondimensional time $ta_0/r_0 \simeq 100$, and steady harmonic wave propagation is achieved after $ta_0/r_0 \simeq 400$ for the case shown in Fig. 4*a*. The intensity of circulation $\Gamma/a_0 r_0 = 1$, the rotating Mach number is $M_r = 0.0796$, the period is $Ta_0/r_0 = 79.05$, and the quadrupole frequency is $fr_0/a_0 = 0.0253$. The result using Thompson's boundary conditions is almost identical to the one using modified boundary conditions until nondimensional time $ta_0/r_0 \simeq 1000$, which correspondings to about 12 periods of rotation. As time marches, the solution using the original Thompson's boundary conditions begins to deteriorate because of the reflected noise. However, the solutions using the presented modified boundary conditions remain stable. A comparison of the acoustic pressure profiles with the theoretical result is shown in Fig. 4*b* along a radial line from the center to the lower-right corner of the domain. It is thought that the Scully vortex model shows more realistic features of the flow, and it is adopted in all of the other results.

### 5.2. Acoustic Fields

As noticed previously, a typical acoustic pressure contour obtained by the method of matched asymptotic expansion is shown in Fig. 2 for the case of the vortex pair of circulation $\Gamma/a_0 r_0 = 1$ and the rotating Mach number is $M_r = 0.0796$. Contour lines are plotted for a range of $-0.0003 \leq p'/\rho_0 a_0^2 \leq 0.0003$ with a step increment of 0.0004. The application of the modified boundary conditions provided highly stable solutions as illustrated in Fig. 4*a*, but the contour lines still have some irregularities over the domain as shown in Fig. 5. The reason for the irregularities is thought to be the discontinuity of vorticity in the Rankine vortex core model. The Rankine model has a discontinuity in vorticity at $r = r_c$ (core radius), whereas the Scully model has a smoothly varying vorticity distribution around the vor-

tex core. The discontinuity of vorticity in space also generates the discontinuity in time for the source terms in the near field. Figures 6*a*-6*c* show the results with the Scully vortex-core model for the same case shown in Fig. 2 and 5. A contour plot for the acoustic pressure is shown in Fig. 6*a*. Fig. 6*b* shows a three-dimensional graphical view of the acoustic pressure exaggerated 200 times.

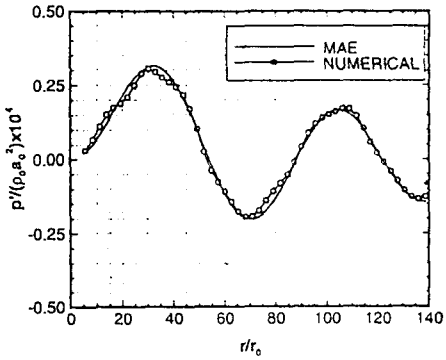


Fig. 7*a* Comparison of acoustic pressure distribution for $\Gamma/a_0r_0 = 0.6, M_r = 0.0477$ with Scully vortex model.

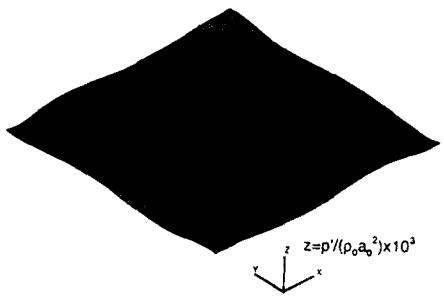


Fig. 7*b* Three-dimensional graphical view of acoustic field for $\Gamma/a_0r_0 = 0.6, M_r = 0.0477$ with Scully vortex model.

A case for a lower rotational frequency is shown in Figs. 7*a* and 7*b*, where the intensity of circulation $\Gamma/a_0r_0$ is 0.6, the frequency is 0.0152, and the rotating Mach number is 0.0477. In Fig. 7*a*, the acoustic pressure profile at an instant along a radial line from the center to the lower-right corner of the domain is compared with the result given by MAE, showing good agreement. Fig. 7*b* is the three-dimensional graphical view of the acoustic field, where the $z$-axis represents 1000 times the acoustic pressure. Fig. 8*a* and 8*b* show a case for a stronger sound source, i.e., higher rotating Mach number, where the intensity of the circulation$\Gamma/a_0r_0 = 1.6$, the frequency $fr_0/a_0$ is 0.0405, and $M_r = 0.1273$. The analytic and numerical acoustic pressure profiles is compared in Fig. 8*a*, and the three-dimensional graphical view of the acoustic field is shown in Fig. 8*b*. The scaling factor of the $z$ axis in Fig. 8*b* is 50.

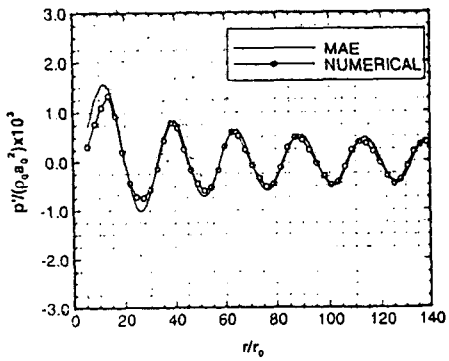


Fig. 8*a* Comparison of acoustic pressure distribution for $\Gamma/a_0r_0 = 1.6, M_r = 0.1273$ with Scully vortex model.

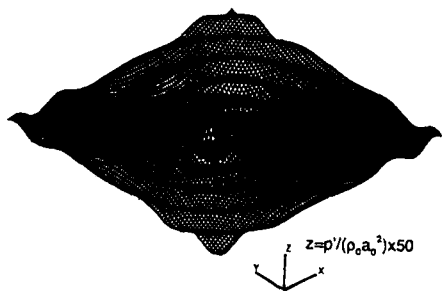


Fig. 8*b* Three-dimensional graphical view of acoustic field for $\Gamma/a_0r_0 = 1.6, M_r = 0.1273$ with Scully vortex model.

It is noticed that the intensity of the sound source is directly related to the rotating Mach number. As theorretically obtained by Müller and Obermeier [2], the intensity of the sound from spinning vortices is proportional to $M_r$ in the compact limit. According to Yates [4], the

compact limit is asymptotically valid for the rotating Mach number $M_r$ less than 0.1. Figures 6*b* and 7*a*, which represent the cases within the compact limit, show good agreements in phase and amplitude compared with the MAE solutions. But, Fig. 8*a* for $M_r = 0.1273$ shows some discrepancy. However, such figures of acoustic pressure profiles do not provide sufficient information to discuss the compactness.

## 6. Conclusion

A computational aeroacoustic technique, which splits Euler equations into hydrodynamic terms and perturbed acoustic terms, is applied to the case of a spinning vortex pair near a flat wall. It is found that the sound generated by the quadrupole source of unsteady vortical flows in the absence of sound-generating body surface (monopole and dipole source) can be calculated by using the source terms due to the hydrodynamic pressure fluctuations. Appropriate modelling of the vortex core is necessary to avoid oscillations of the solutions to the problems considered. The Scully vortex-core model shows better results than Rankine model. Nonreflecting boundary conditions are developed to obtain highly stable solutions.

## References

[1] Powell, A., "Theory of Vortex Sound," *Journal of the Acoustical Society of America*, Vol. 36, No. 1, (1964), pp. 177-195

[2] Müller, E.A., and Obermeier, F., "The Spinning Vortices as a Source of Sound," AGARD CP-22, (1967), pp. 22.1-22.8

[3] Obermeier, F., "The Application of Singular Perturbations Methods to Aerodynamic Sound Generation," *Singular Perturbations and Boundary Layer Theory*, edited by Brouner, Gray and Mathieu, Springer-Verlag, Berlin, (1977), pp. 401-421

[4] Yates, J.E., "Application of the Bernoulli Enthalpy Concept to the Study of Vortex Noise and Jet Impingement Noise," NASA CR2987, (1978)

[5] Möhring, W., "On Vortex Sound at Low Mach Number," *Journal of Fluid Mechanics*, Vol. 85, (1978), pp. 685-691

[6] Kambe, T., "Acoustic Emissions by Vortex Motions," *Journal of Fluid Mechanics*, Vol. 173, (1986), pp. 643-666.

[7] Colonius, T., Lele, S.K., and Moin, P., "Scattering of Sound Waves by a Compressible Vortex," AIAA Paper 91-0494, (1991)

[8] Mitchell, B.E., Lele, S.K., and Moin, P., "Direct Computation of the Sound from a Compressible Co-rotating Vortex Pair," AIAA Paper 92-0374, (1992)

[9] Huh, K.S., Agrawal, R.K., and Widnall, S. E., Numerical Simulation of Acoustic Diffraction of Two-dimensional Rigid Bodies in Arbitrary Flows," AIAA Paper 90-3920, (1990)

[10] Watson, W.R., and Myers, M.K., "A Two-step Method for Evolving Acoustic Systems to a Steady-state," AIAA Paper 90-3946, (1990)

[11] Hardin, J.C., and Pope, D.S., "Sound Generated by a Stenosis in a Pipe," AIAA Paper 90-3919, (1990)

[12] Hardin, J. C., and Pope, D.S., "A New Technique for Aerodynamic Noise Calculation," DGLR/AIAA 92-02-076, (1992)

[13] Lee, D.J. and Koo, S.O., "Numerical Study of Sound Generation Due to a Spinning Vortex Pair," *AIAA Journal* Vol. 33, No. 1, (1995), pp. 20-26

[14] Koo, S.O., "Numerical Study of Acoustic Fields Generated by Unsteady Vortical Flows," Ph.D. Thesis, KAIST, (1995)

[15] Thompson, K.W., "Time Dependent Boundary Conditions for Hyperbolic Systems," *Journal of Computational Physics*, Vol. 68, (1987), pp. 1-24

[16] Scully, M.P., "Computational of helicopter Rotor Wake Geometry and Its Influence on Rotor Harmonic Airloads," MIT, Pub. ARSL TR 178-1, Cambridge, MA, March, (1975)

[17] Anderson, D.A., Tannehill, J.C., and Pletcher, R.H., *Computational Fluid Mechanics and Heat Transfer*, McGraw-Hill, New York, (1984)